Effects of Emergent Grass on Mid-Infrared Laser Reflectance of Soil

Ram M. Narayanan and Brian D. Guenther

Abstract

Mid-infrared laser reflectances of soils containing specific minerals show diagnostic features in the 9- to 11-μm wavelength range, and are thus useful for remote sensing of terrestrial lithology. However, the presence of actively growing vegetation can obscure these diagnostic features to such an extent as to make mineral identification virtually impossible. The effects of emergent grass on the mid-infrared laser reflectance of bare soil were studied experimentally. Speckle-averaged reflectance data were collected at various wavelengths, incidence angles, and polarization combinations from a large movable soil container. Initial measurements were made on bare soil under various wetness and surface roughness conditions. Grass was then grown on the soil, and three different grass densities were used in different sub-plots of the container. Reflectance data were gathered from each sub-plot as the grass-blade height increased. Reflectance ratios (indicative of diagnostic features) were plotted as a function of grass-blade height for different grass densities. There appeared a grass-blade height value at which the diagnostic ratios level off to a value of 1.0, thereby masking the underlying soil reflectance features. These results should be useful for identifying optimal conditions under which soil mineralogy can be identified under overlying vegetation using mid-infrared laser spectroscopy.

Introduction

Mid-infrared spectroscopy has emerged as a powerful tool for monitoring terrestrial lithology by making use of the unique spectral features of various minerals and mineral-bearing soils in this wavelength range (Salisbury *et al.*, 1987; Bartholomew *et al.*, 1989; Salisbury *et al.*, 1991). Although a majority of the reflectance measurements were initially made using passive spectroradiometers, CO_2 lasers have been increasingly used to improve the signal-to-noise ratio, to achieve better resolution, and to characterize the angular and polarization dependence of the reflectance (Shumate *et al.*, 1982; Becker *et al.*, 1985; Eberhardt *et al.*, 1985; Cvijin *et al.*, 1987; Narayanan *et al.*, 1992a). Airborne CO_2 laser spectrometer systems have been developed and tested for characterizing the reflectance of terrain for identification and discrimination purposes under potentially operational conditions (Wiesemann *et al.*, 1978; Bufton *et al.*, 1982; Kahle *et al.*, 1984; Whitbourn *et al.*, 1990). Recent attempts to make calibrated field measurements of laser reflectance of terrain targets have proved successful, and the data agreed qualitatively and quantitatively with controlled laboratory measurements on small samples (Narayanan and Green, 1994). These developments lead us to believe that compact mid-infrared laser sensors can be flown on airborne platforms in the near future for rapid identification and delineation of surficial mineralogy. Such a system would be useful not only in terrestrial studies but, more importantly, also in planetary investigations.

Although the potential for mineral identification using mid-infrared spectroscopy has been established in the laboratory and under controlled experiment conditions, rarely are such ideal situations ever available under realistic operational scenarios. Mineral-bearing soils are usually mixed with vegetation of different types, densities, and heights. The presence of vegetation adds its own fingerprint to the spectral characteristics of soil, and can completely mask the soil reflectance if the vegetative cover is tall and dense. Even under sparse vegetation conditions, the composite reflectance of a pixel containing soil and vegetation is different from that containing bare soil alone, and the degree of departure from the soil reflectance depends largely on the type and amount of vegetation in the pixel, as well as whether the vegetation is live or dead (Siegal and Goetz, 1977; Murphy, 1995). Reflectance measurements of individual leaves, both green and dry, in the mid-infrared spectral region have shown generally featureless characteristics, i.e., absence of sharp peaks or troughs, as well as lower reflectance values compared to soils (Elvidge, 1988; Salisbury and Milton, 1988; Narayanan *et al.*, 1990; Narayanan *et al.*, 1992c). This confounds the identification of specific minerals in the soil based on metrics derived from the spectral characteristics, such as wavelength of maximum absorption, height or depth of absorption features, ratio of reflectance at specific wavelengths, etc.

This paper describes the results of an experimental study to characterize the effects of emergent grass cover on the mid-infrared laser reflectance of soil. The soil reflectance was measured under different conditions of surface roughness and soil moisture in order to establish an appropriate baseline for comparison. Reflectance measurements on soil under various conditions of emergent grass cover, such as grass height and grass density, were then made to assess its effect on soil reflectance. The next section describes the experimental setup used for the study, and is followed by a section that presents and discusses the measured data on both bare and grass-covered soil. Conclusions and directions for future work in this area are presented at the end.

Department of Electrical Engineering, Center for Electro-Optics, University of Nebraska, Lincoln, NE 68588-0511 (rnarayanan@unl.edu).

B.D. Guenther is presently with J.A. Woollam Co., Inc., Lincoln, NE 68508.

Photogrammetric Engineering & Remote Sensing, Vol. 64, No. 5, May 1998, pp. 407–413.

0099-1112/98/6405–407$3.00/0

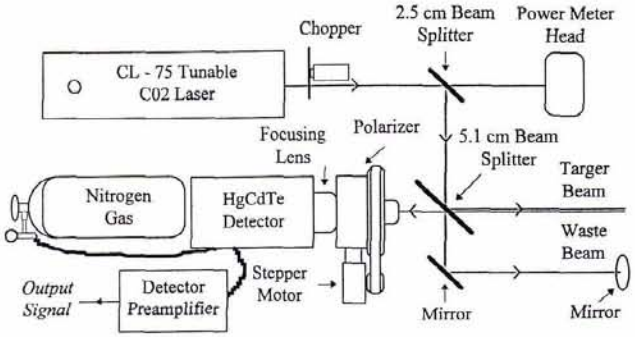

Figure 1. Block diagram of the 9- to 11-μm laser reflectance sensor.

Materials and Methods

Laser Reflectance Sensor System Description

The laser reflectance sensor used for these measurements consists of a line-tunable CO_2 laser that is tunable over the 9- to 11-μm wavelength range. It has an output power of 5.5 W minimum, a beam divergence of 8 mrad, and an output polarization purity of better than 600:1. The receiver consists of a lens-detector combination with a field of view (FOV) of 17 mrad, followed by a matched preamplifier and a lock-in amplifier. A 10,000:1 extinction ratio polarizer is used before the receiver to select co-polarized or cross-polarized backscattered energy. The entire system is housed in an enclosure that has overall dimensions of approximately 104 cm by 38 cm by 22 cm. A simplified block diagram showing the physical layout of the optical components is shown in Figure 1. This part of the system is described in greater detail in Narayanan and Green (1994).

The block diagram of the data acquisition system is shown in Figure 2. The output signal from the lock-in amplifier is fed to the digital oscilloscope as well as to a multifunction analog-to-digital (A/D) conversion board. The A/D board is housed in a laptop docking station used with a notebook computer. An IEEE-488 bus is used for instrument control and data acquisition. A specially designed triggering circuit is used to trigger the multifunction board during data acquisition.

Measurements were made at four wavelengths in the mid-infrared range, and at three incidence angles. Although both co-polarized and cross-polarized reflectance measurements were made, only the co-polarized reflectivity was analyzed further. The system operating conditions are listed in Table 1. Thus, for each target condition, a total of 12 measurement sets were obtained (four wavelengths by three angles by one polarization).

TABLE 1. SYSTEM OPERATING CONDITIONS

Parameter	Value
Wavelengths (μm)	9.283, 9,520, 10.247, 10.633
Incidence angles (°)	0, 20, 50
Polarization	Co-Polarized

The laser sensor assembly is placed on the optical table, and the beam is directed to the bare or grass-covered soil target using an adjustable mirror to vary the angle of incidence, as shown in Figure 3. The waste beam (emerging from the 5.1-cm beamsplitter shown in Figure 1) is directed at the 5-m-high ceiling, and our measurements indicate that the reflected energy, if any, from the waste beam is small compared to the reflected energy from the soil target.

Calibration is performed using a Labsphere Infragold 94 percent diffuse reflectance standard. This standard was one of many that were independently measured by various laboratories, the results of which are summarized by Willey (1987). Based on those measurements, we compute the mean reflectance as 0.944 and the standard deviation as 0.036 in the 9- to 11-μm range. It must be pointed out, however, that various Infragold samples have shown as much as 4 percent variation in absolute reflectance values. Immediately following the measurement of the reflected power from the sample for each unique wavelength, incidence angle, and polarization combination, a measurement was also made of the power reflected by the calibration target in order to account for any long-term power-output drifts of the laser. A normalized reflectance is computed for each sample by taking the ratio of the reflected intensity from the sample at the specified polarization and incidence angle to the co-polarized normal-incidence reflected intensity from the calibration standard.

Movable Soil Container

The movable soil container is attached to a carriage whose linear translation is governed by a variable speed motor. The translation is necessary in order to obtain uncorrelated reflectance samples for speckle averaging. The speed of translation is monitored using an optical switch. The soil container is constructed out of a 244-cm (8-ft) by 122-cm (4-ft) piece of 1.9-cm (3/4-in) thick plywood with a 6.4-cm (2.5-in) by 3.8-cm (1.5-in) lip around the outside edge on top of the plywood sheet to form the storage area for the soil. The soil container

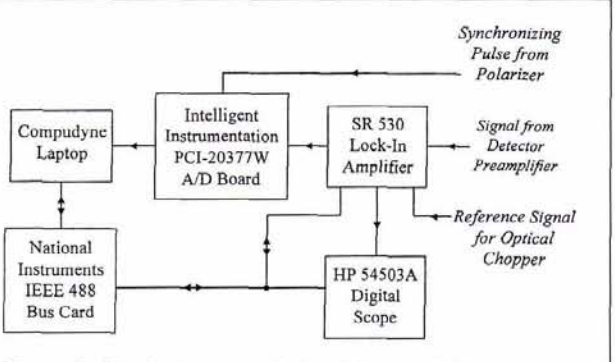

Figure 2. Block diagram of the data acquisition system.

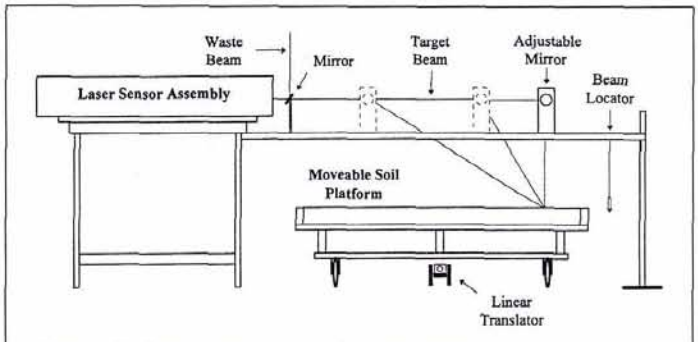

Figure 3. Arrangement showing incidence angle adjustment.

is 225 cm long, 112 cm wide, and 6.4 cm deep. Adequate support is provided for the plywood to prevent bending or breakage when the soil is added. The container is divided into three equally sized areas along its length, each area being approximately 75 cm long and 112 cm wide. The speed of the soil container is adjusted so that each reflectance sample, obtained by chopping the laser beam, is uncorrelated. This is accomplished by translating the container with a speed such that the spacing between each sample is greater than the largest spot size illuminated, which is about 16 mm.

Preparation of Bare and Grass-Covered Soil

The soil used for our measurements was a clayey topsoil provided by a local construction company. The soil contained quartz as its major mineral constituent. In order to set the appropriate baseline of soil reflectance data, measurements were made on the soil under different gravimetric moisture and surface macro-roughness conditions. To vary the soil moisture, the soil was first completely saturated and made to attain its maximum moisture content value. Water was added using a multipurpose sprayer, and the soil was thoroughly mixed continuously as water was added, thus ensuring that the soil moisture distribution was uniform. The soil container was covered by an airtight plastic sheet so as to allow the system to equilibrate for two days, with daily mixing of the soil to ensure a homogeneous distribution of soil moisture. It was only after this operation that the soil reflectance data were gathered. Corresponding gravimetric soil moisture was measured at nine different locations to characterize the variability in this parameter. To attain a lower soil moisture, the plastic cover was removed for a day to allow some of the moisture to evaporate. The same procedure, i.e., airtight sealing, mixing, and two-day waiting, was repeated to ensure a uniform soil moisture distribution, and reflectance data and the actual gravimetric soil moisture data were recorded. This procedure was repeated until the lowest soil moisture was attained. A total of ten gravimetric soil moisture values ranging between 22.5 gm/cc and 7.9 gm/cc were attained in this manner. Values lower than 7.9 gm/cc could not be consistently maintained due to the hygroscopic nature of the soil. The standard deviation of the nine measurements for each moisture value varied between 0.29 gm/cc and 0.84 gm/cc, thereby indicating that the moisture distribution was indeed uniform.

To vary the soil macro roughness, we took advantage of the soil clodding process during wetting. The clods were sorted into different parts of the soil container during the preparation of the highest soil moisture value. Two sieves of size 0.64 cm and 1.3 cm were constructed using appropriate hail screens mounted on 45.7-cm-square wooden frames. Clods were sieved through the smaller hail screen first. Those that fell through (sizes smaller than 0.64 cm) were used for the light roughness soil. The clods were then sieved through the larger hail screen, and those that fell through (sizes between 0.64 cm and 1.3 cm) were used for the medium roughness soil. Clods that remained in the larger sieve (size larger than 1.3 cm) were used for the heavy roughness soil. It is to be emphasized here that all three soil roughness conditions were considered "electromagnetically rough" with respect to the short (~ 10-μm) wavelength of the laser beam. Each of the three soil roughnesses was induced in each of the three 75- by 112-cm areas in the container.

In order to understand the effects of vegetation on the reflectance characteristics of soil, Kentucky 31 Tall Fescue grass was planted in each of the three 75- by 112-cm areas in the container. The grass seed was chosen on the basis of its relatively short germination time compared to others available locally. Once the seeds were planted, the grass blades emerged from the soil within five days. The density of grass seeds planted in each of the three areas mentioned above was varied using a Scotts Accugreen gravity flow spreader, which had a 53-cm width and a variable output dial ranging from 2 (very light) to 18 (heavy). The spreader settings used were 6 for light density, 12 for medium density, and 18 for heavy density vegetation. The grass seed was spread on top of a 4-cm layer of lightly packed soil of approximately 18 percent soil moisture, which was then covered by a 0.5-cm layer of smooth soil, and finally topped by inducing medium roughness on the soil surface. The soil was then covered with a clear plastic sheet held by a small support structure to make a small greenhouse. The grass seed was planted on 2 July 1994, and grass was emergent on 8 July. The underlying soil moisture was measured at three locations in each area to ensure that the moisture distribution was uniform during the measurements on grass-covered soil.

Reflectance Characteristics

Bare Soil

A total of 12 data files were collected for bare soil. As mentioned before, bare soil gravimetric moisture values varied between 7.9 and 22.5 gm/cc; thus, it was not possible to study the reflectance of dry soil. For each moisture value, reflectance data were collected from all three surface roughness treatments, i.e., light, medium, and very rough. It was found that there was no observable dependence on the surface macro roughness. This was somewhat expected owing to the "electromagnetically very rough" nature of the soil. It was also found that the normalized reflectance decreased with increasing moisture. This observation was consistent with our earlier controlled measurements (Narayanan *et al.*, 1993), based on which a negative exponential dependence on soil moisture was postulated. Our current measurements showed more variability, and we fitted a simpler linear relationship to describe the reflectance dependence on soil moisture using data from all macro roughness treatments. The linear model was of the form

$$\rho(\lambda, \theta, m_g) = \rho_0 - a m_g \qquad (1)$$

where ρ is the normalized reflectance, λ is the wavelength, θ is the incidence angle, m_g is the moisture content in percent, and ρ_0 and a are best-fit constants. It is to be noted that the linear model is only applicable within the moisture range used to develop the model, and extrapolation to values outside the range may not yield accurate reflectance estimates. In general, the R^2 values of the fits were low, but the linear dependence is clearly seen in Figures 4 and 5. Figure 4 shows the dependence of normalized reflectance on moisture at the 9.283-μm wavelength for the three angles of incidence, while Figure 5 shows the same plots at the 10.633-μm wavelength. The best-fit parameters are shown in Table 2 for all wavelengths at incidence angles of 20° and 50°. The reflectance at 0° incidence was dominated by a large specular component that was very sensitive to aspect; hence, we did not attempt to fit a straight line to this data set. It is also observed that the ρ_0 value is lower in the 10-μm wavelength range compared to the value in the 9-μm range, especially the 9.283-μm wavelength, and this is expected due to the fact that the major mineral constituent in the soil is quartz.

Vegetation-Covered Soil

A total of six data files were collected from the grass-covered soil, one on each different day. The underlying soil moisture was also measured at three locations each time, and the daily mean values ranged between 18.1 percent and 19.4 percent, with standard deviations of the order of 0.6 percent. This amount of underlying soil moisture was necessary in order to keep the grass growing. In order to quantify the grass

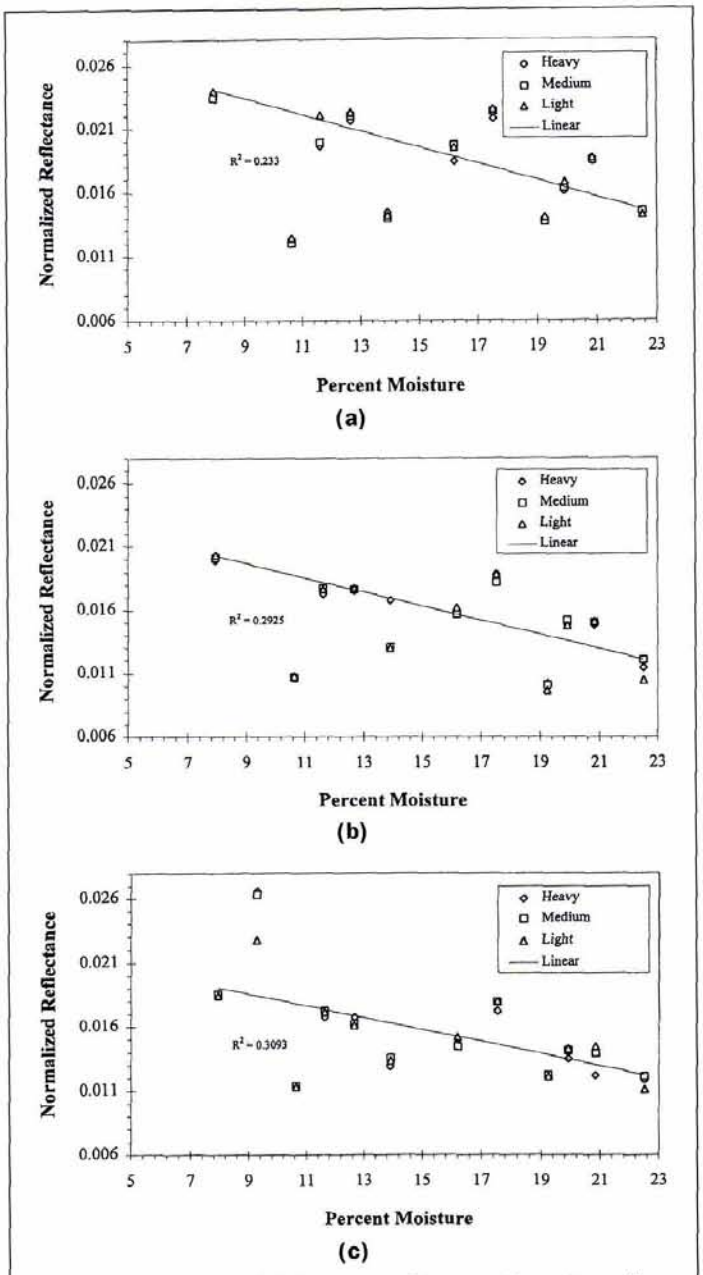

Figure 4. Normalized reflectance of bare soil versus soil moisture at 9.283 μm at incidence angles of (a) 0°, (b) 20°, and (c) 50°.

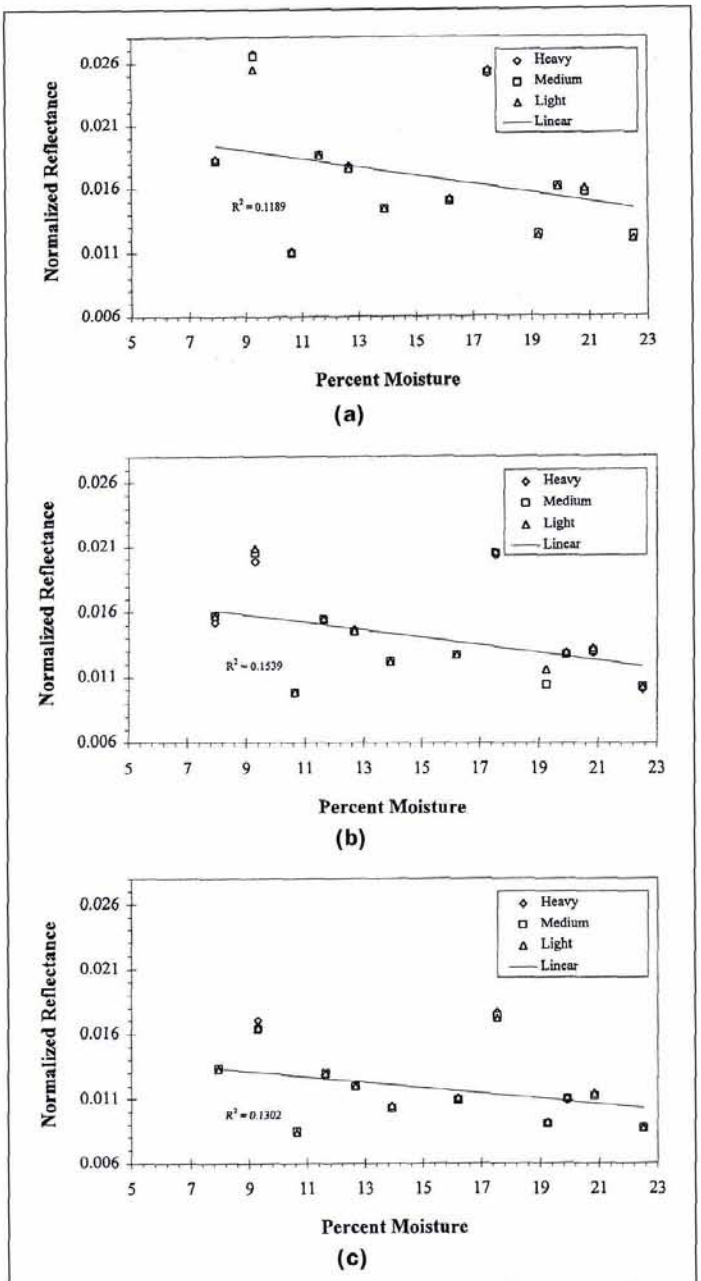

Figure 5. Normalized reflectance of bare soil versus soil moisture at 10.633 μm at incidence angles of (a) 0°, (b) 20°, and (c) 50°.

density, the number of grass blades per unit area was measured for all three densities, and these values are listed in Table 3. Average grass-blade height was also measured each day, and these values ranged from 0 cm (pre-emergent) to 10.8 cm (fully grown). A typical plot showing the variation of normalized reflectance at the 9.283-μm wavelength with grass-blade height for various grass densities and incidence angles is shown in Figure 6. Note that the value of the nor-

TABLE 2. BEST-FIT PARAMETERS FOR SOIL NORMALIZED REFLECTANCE

Wavelength (μm)	Incidence Angle (°)	ρ_0	a
9.283	20	0.0248	6.02×10^{-4}
	50	0.0228	5.16×10^{-4}
9.520	20	0.0236	3.32×10^{-4}
	50	0.0214	5.86×10^{-4}
10.247	20	0.0191	0.72×10^{-4}
	50	0.0158	3.26×10^{-4}
10.633	20	0.0184	3.19×10^{-4}
	50	0.0150	2.27×10^{-4}

TABLE 3. GRASS BLADE DENSITY VALUES

Spreader Setting	Grass Blade Density (m^{-2})
6 (Light)	2500
12 (Medium)	3800
18 (Heavy)	7400

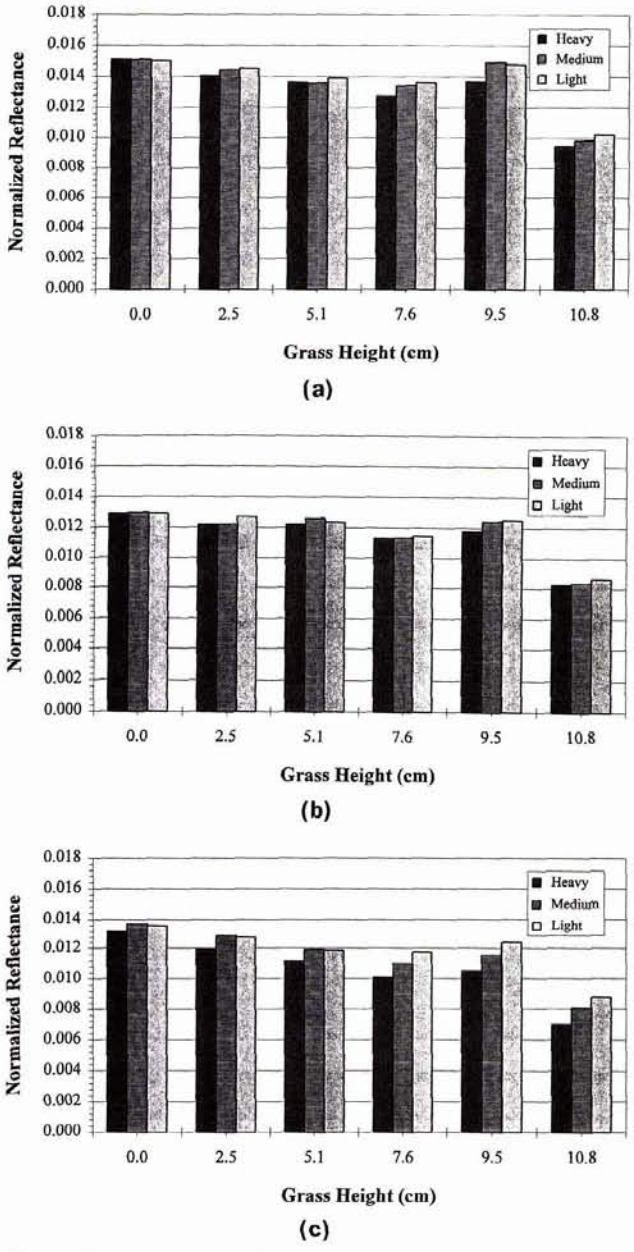

Figure 6. Normalized reflectance of grassy soil versus grass height at 9.283 μm at incidence angles of (a) 0°, (b) 20°, and (c) 50°.

malized reflectance for 0 cm height (pre-emergent) is consistent with the value seen in Figure 4 for approximately 18.5 percent soil moisture obtained from prior bare soil measurements. It is observed that the reflectance of grass-covered soil decreases with increasing grass blade height, and the decrease is highest for heavy density grass and lowest for light density grass. This is entirely expected because higher grass densities and blade heights indicate higher biomass within the probing beam which, in turn, yields a lower reflectance value.

The effect of grass height on normalized reflectance is not very significant at 0° incidence, as can be seen in Figure 6(a). On the other hand, the lowering of reflectance with increasing grass blade height can be clearly observed at 50° incidence. We attribute this to the viewing angle geometry effect, as shown in Figure 7, wherein we have modeled the grass blades as vertical cylinders, an assumption that is valid for Kentucky 31 Tall Fescue. As can be seen, there is no change in the amount of grass biomass within the probing beam at normal incidence as the grass grows taller, but this is not true at oblique incidence, such as at 50°. The large drop in the reflectance at 0° incidence for a grass height of 10.8 cm is attributed to the fact that, at or near this height, the grass blade starts to curl and bend, and this lowers the reflectance because more of the grass appears within the probing beam, thereby obscuring more of the higher reflectance soil surface. Although Figure 6 shows the dependence of reflectance on grass height at the 9.283-μm wavelength, similar effects were apparent at the other three wavelengths used in the study.

One of the metrics widely used for mineral identification and soil discrimination is a reflectance ratio obtained from reflectance measurements at judiciously selected wavelengths (Shumate *et al.*, 1982; Narayanan *et al.*, 1992b). This metric has the advantage of not requiring absolute calibration if the system transfer function and the propagation characteristics of the intervening atmosphere are independent of the probing wavelengths. The choice of wavelengths is crucial in obtaining the required sensitivity for discrimination. In general, mineral-bearing soils have unique absorption features in the 9- to 11-μm wavelength range, while green vegetation is usually featureless. Thus, we expect a reflectance ratio formed using reflectance measurements at the wavelength of maximum reflectance to the wavelength of low reflectance to correlate well with vegetation biomass. This conjecture is based on the fact that such a reflectance ratio will be high (greater than unity) for bare soil and nearly equal to unity for dense vegetation, with intermediate values depending upon the vegetation density. We explored the dependence of six such reflectance ratios (derived from our measurements at four wavelengths) on the grass height, and concluded that the best sensitivity and correlation with grass height was obtained by using measurements at the 9.283 and 10.633-μm wavelengths. This is not surprising because quartz, the major soil mineral, has a peak near 9 μm, and lower reflectance values in the 10-μm region; thus, this ratio is expected to be high for bare soil. This ratio was approximately equal to 1.32 under all soil macro-roughness and moisture conditions at 50° incidence.

Plots showing the dependence of the reflectance ratio described above as a function of grass blade height for various grass densities are shown in Figure 8. These plots are shown at 50° incidence, at which the sensitivity was maximum. In these plots, the reflectance ratio of the bare soil, using data collected during the bare soil experimentation phase, is also indicated (at 0 cm blade height), and it is reassuring to note that these values are close to the measurements made after the grass seeds were planted during the vegetation experi-

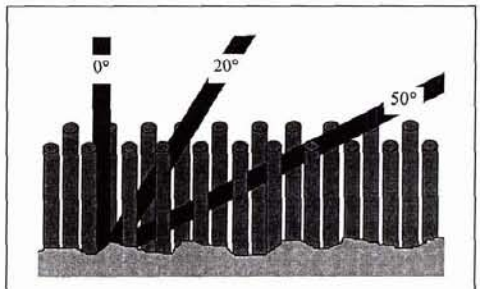

Figure 7. Viewing angle geometry.

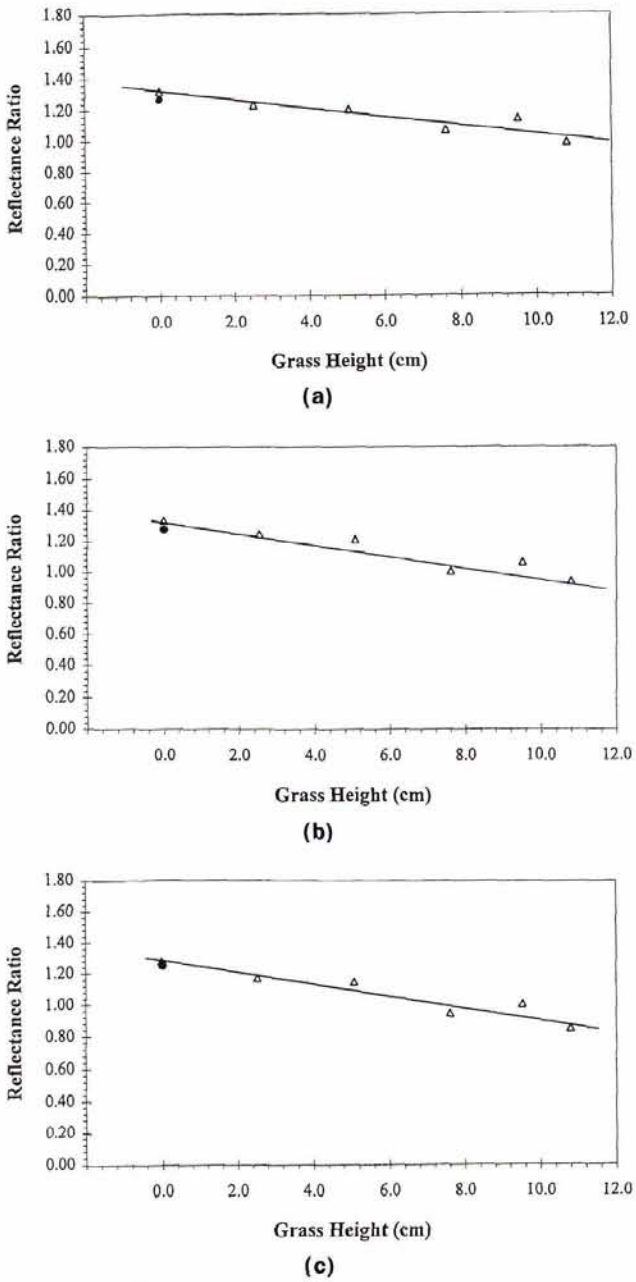

Figure 8. Reflectance ratio versus grass-blade height for (a) light density grass, (b) medium density grass, and (c) high density grass. Circle represents ratio for bare soil.

mentation phase. We also note that the ratio is almost the same for each grass density measurement under pre-emergent conditions, i.e., at 0 cm grass-blade height. We observe from the plots that the reflectance ratio drops off linearly from its value at 0 cm, and reaches the value of unity at a grass height value that depends on the grass density; the higher the density, the lower the grass height at which this ratio reaches unity, thus effectively obscuring the underlying soil reflectance features. This dependence is modeled as a linear function given by

$$R(h,d) = R(0,d) - b(d)h \qquad (2)$$

where $R(h,d)$ is the reflectance ratio, h is the grass height, d is the grass density, and $b(d)$ is the (negative) slope of the curve. Values of $R(0,d)$ and $b(d)$ are listed in Table 4, from which we note that $b(d)$ is expectedly higher for higher density.

TABLE 4. BEST-FIT VALUES OF $R(0,d)$ AND $b(d)$ FOR DIFFERENT GRASS DENSITIES

Grass Density	$R(0,d)$	$b(d)$
Light	1.326	0.0279
Medium	1.341	0.0390
Heavy	1.305	0.0400

While the value of $R(0,d)$ is approximately the same for all grass density values, the slope $b(d)$ appears to have an increasing but saturating relationship with respect to grass-blade density. An increase in blade density from 2500 m^{-2} to 3800 m^{-2}, i.e., a factor of 1.52, causes an increase in $b(d)$ from 0.0279 to 0.0390, i.e., a factor of 1.40. However, an increase in blade density from 3800 m^{-2} to 7400 m^{-2}, i.e., a factor of 1.95, causes in increase in $b(d)$ from, 0.0390 to 0.0400, i.e., a factor of only 1.026. This suggests that a simple surface scattering model is not adequate to describe the reflectance of the soil-vegetation system, and one must consider multiple scattering as well as the interaction between the soil and the vegetation in order to explain the saturating trend of the (negative) slope of the reflectance ratio with respect to grass height.

Equation 2 can be recast into an appropriate form to determine the value of grass height, h^*, at which R attains the value of unity, i.e., at which $R(h^*, d) = 1$. This is given by

$$h^* = \frac{R(0,d) - 1}{b(d)} \qquad (3)$$

from which the inverse relationship between h^* and $b(d)$ is more clearly seen. The value of h^* is computed as 11.7 cm for light density grass, 8.7 cm for medium density grass, and 7.6 cm for high density grass.

Conclusions

Our study indicates that actively growing vegetation obscures the spectral characteristics of mineral-bearing soils in the mid-infrared region of the electromagnetic spectrum. The degree of obscuration increases with vegetation height and vegetation density. This indicates that actively growing vegetation can confound the remote determination of mineral-bearing soils under high biomass conditions. Although our study deals with one particular type of grass over one particular type of soil, we postulate that similar results would be obtained for other cases. This calls for a more detailed study involving further experimentation and analysis over a wider variety of vegetation and soil types.

Acknowledgments

The technical assistance of Steven E. Green of the J.A. Woollam Co., Inc. is gratefully acknowledged.

References

Bartholomew, M.J., A.B. Kahle, and G. Hoover, 1989. Infrared spectroscopy (2.3-20 μm) for the geological interpretation of remotely-sensed multispectral thermal infrared data, *International Journal of Remote Sensing*, 10(3):529–544.

Bufton, J.L., T. Itabe, and D.A. Grolemund, 1982. Dual-wavelength correlation measurements with an airborne pulsed CO_2 laser system, *Optics Letters*, 7(12):584–586.

Becker, F., P. Ramanantsizehena, and M.P. Stoll, 1985. Angular vari-

ation of the bidirectional reflectance of bare soils in the thermal infrared band, *Applied Optics*, 24(3):365–375.

Cvijin, P.V., D. Ignjatijevic, I. Mendas, I. Sreckovic, L. Pantani, and I. Pippi, 1987. Reflectance spectra of terrestrial surface materials at CO_2 laser wavelengths: Effects on DIAL and geological remote sensing, *Applied Optics*, 26(19):4323–4329.

Eberhardt, J.E., J.G. Haub, and A.W. Pryor, 1985. Reflectivity of natural and powdered minerals at CO_2 laser wavelengths, *Applied Optics*, 26(3):388–395.

Elvidge, C.D., 1988. Thermal infrared reflectance of dry plant materials: 2.5-20 μm, *Remote Sensing of Environment*, 26(3):265–285.

Kahle, A.B., M.S. Shumate, and D.B. Nash, 1984. Active airborne infrared laser system for identification of surface rock and minerals, *Geophysical Research Letters*, 11(11):1149–1152.

Murphy, R.J., 1995. The effects of surficial vegetation cover on mineral absorption feature parameters, *International Journal of Remote Sensing*, 16(12):2153–2164.

Narayanan, R.M., S.E. Green, and D.R. Alexander, 1990. Mid-infrared backscatter spectra of selected agricultural crops, *Proc. SPIE Conference on Optics in Agriculture*, Boston, Massachusetts, 1379:116–122.

Narayanan, R.M., S.E. Green, and D.R. Alexander, 1992a. Mid-infrared backscatter characteristics of various benchmark soils, *IEEE Transactions on Geoscience & Remote Sensing*, 30(5):516–530.

Narayanan, R.M., S.E. Green, and D.R. Alexander, 1992b. Soil classification using mid-infrared off-normal active differential reflectance characteristics, *Photogrammetric Engineering & Remote Sensing*, 58(2):193–199.

Narayanan, R.M., L.N. Mielke, and T.J. Schirmer, 1992c. Mid-infrared laser reflectance of crop leaves subjected to water stress, *Proc. International Geoscience and Remote Sensing Symposium*, Houston, Texas, pp. 339–341.

Narayanan, R.M., S.E. Green, and D.R. Alexander, 1993. Mid-infrared laser reflectance of moist soils, *Applied Optics*, 32(30):6043–6052.

Narayanan, R.M., and S.E. Green, 1994. Field measurements of natural and artificial targets using a mid-infrared laser reflectance sensor, *IEEE Photonics Technology Letters*, 6(8):1023–1026.

Salisbury, J.W., and N.M. Milton, 1988. Thermal infrared (2.5 to 13.5 μm) directional hemispherical reflectance of leaves, *Photogrammetric Engineering & Remote Sensing*, 54(9):1301–1304.

Salisbury, J.W., L.S. Walter, and N. Vergo, 1987. *Mid-Infrared (2.1-25 μm) Spectra of Minerals, First Edition*, U.S. Geological Survey Open File Report 87-263.

Salisbury, J.W., D.M. D'Aria, and L.E. Brown, 1991. *Infrared (2.08-14 μm) Spectra of Soils: A Preliminary Report*, Johns Hopkins University.

Shumate, M.S., S. Lundquist, U. Persson, and S.T. Eng, 1982. Differential reflectance of natural and man-made materials at CO_2 laser wavelengths, *Applied Optics*, 21(13):2386–2389.

Siegal, B.S., and A.F.H. Goetz, 1977. Effect of vegetation on rock and soil type discrimination, *Photogrammetric Engineering & Remote Sensing*, 43(2):191–196.

Whitbourn, L.B., R.N. Phillips, G. James, M.T. O'Brien, and M.D. Waterworth, 1990. An airborne multiline CO_2 laser system for remote sensing of minerals, *Journal of Modern Optics*, 37(11): 1865–1872.

Wiesemann, K., R. Beck, W. Englisch, and K. Gurs, 1978. In-flight test of a continuous laser remote sensing system, *Applied Physics*, 15(3):257–260.

Willey, R.W., 1987. Results of a round robin measurement of spectral emittance in the mid-infrared, *Proc. SPIE Conference on Passive Infrared Systems and Technology*, The Hague, Netherlands, 807:140–147.

(Received 25 February 1997; accepted 5 November 1997)